Available online at www.sciencedirect.com
ScienceDirect
Journal of the European Ceramic Society 26 (2006) 3431–3440
www.elsevier.com/locate/jeurceramsoc

Effects of $CaCO_3$ content on the densification of aluminum nitride

A.L. Molisani [a], H.N. Yoshimura [a,*], H. Goldenstein [b], K. Watari [c]

[a] *Institute for Technological Research of the State of São Paulo, Av. Prof. Almeida Prado, 532, São Paulo, SP 05508-901, Brazil*
[b] *Polytechnic School of the University of São Paulo, Av. Prof. Mello Moraes, 2463, São Paulo, SP 05508-900, Brazil*
[c] *National Institute of Advanced Industrial Science and Technology, Ceramics Research Institute, Moriyama-Ku, Nagoya 463-8560, Japan*

Received 11 May 2005; received in revised form 8 August 2005; accepted 14 August 2005
Available online 19 October 2005

Abstract

The effect of adding up to 13.4 wt.% $CaCO_3$ on the densification behavior of aluminium nitride (AlN) was investigated during pressureless sintering between 1100 and 2000 °C. The presence of second-phases, weight losses, Ca contents, and microstructures of sintered samples were correlated with the densification curves. Two microstructural aspects determined the densification of aluminum nitride with $CaCO_3$: second-phase evolution path and formation of large pores. Additions of small amounts of $CaCO_3$ caused the formation of higher melting point calcium aluminates (mainly CA_2) that increased the temperature at which liquid-phase sintering process started, but once activated rapid densification was observed. For larger $CaCO_3$ amounts, liquid-phase started to form at lower temperature, but the initial densification was slow, diminishing the advantage of lower $C_{12}A_7$ related eutectic temperature. Irrespective of the initial $CaCO_3$ content, all second-phase evolution paths converged to CA phase above 1600 °C, suggesting that during sintering of AlN with CaO at high temperatures, a liquid phase with composition of CA phase is more stable than others compositions. The effect of this composition changing on densification is discussed. Large pores were formed in the sites originally occupied by large particles of $CaCO_3$ and retarded the bulk densification in samples with high additive contents.

Keywords: AlN; Porosity; Sintering; Microstructure-final; Substrates

1. Introduction

Aluminum nitride (AlN) has attracted attention of the electronic device industries because of its excellent properties, such as high thermal conductivity, thermal expansion matching that of silicon, good electrical insulation, low dielectric constant, and non-toxicity.[1] AlN recently emerged as a favorable candidate to replace aluminum oxide (Al_2O_3) and beryllium oxide (BeO) in the manufacture of semiconductor devices.[2] Some of its main applications are substrates for power transistors and high frequency devices, device packages for large-scale integration (LSI) and very large-scale integration (VLSI), laser components, and insulators with high thermal conductivity for thyristors.

AlN can be pressureless sintered with the aid of additives, which react with the alumina layer on the surface of the AlN particles forming aluminates that promote densification by liquid-phase sintering.[3,4] The use of aluminate forming additives, like Y_2O_3 and CaO, has the additional benefit of fixing the superficial alumina in the second-phases at the grain boundaries, lowering the oxygen content in solution in the AlN lattice.[4] Oxygen in solution is the main factor that affects the thermal conductivity of AlN, as it causes the formation of Al vacancies, which scatter phonons.[5] Y_2O_3 is the most used additive for production of high thermal conductivity AlN, but it requires the use of high sintering temperatures (1800 °C or above).[6] Efforts have been made to lower the sintering temperature of AlN, which could be beneficial to co-firing of multilayer substrates, besides reducing manufacturing costs, and improving mechanical properties. Although CaO additions generally result in AlN with lower thermal conductivity than Y_2O_3,[7,8] it has the advantage of diminishing the sintering temperature. Processing of AlN with Y_2O_3 and CaO are well-established techniques, although the sintering mechanisms involved are not clear yet.

Komeya et al.[9] sintered AlN with 0.5–5 wt.% $CaCO_3$ at 1700 °C and observed increasing relative densities (from 72 to 97%) with increasing $CaCO_3$ content. They proposed that this result was related to the *liquidus* temperature of the second-phases formed, CA ($CaO{\cdot}Al_2O_3$) in 5 wt.% $CaCO_3$ sample and

* Corresponding author. Tel.: +55 11 3767 4549; fax: +55 11 3767 4561.
E-mail address: hnyoshim@ipt.br (H.N. Yoshimura).

0955-2219/$ – see front matter © 2005 Elsevier Ltd. All rights reserved.
doi:10.1016/j.jeurceramsoc.2005.08.010

CA_6 ($CaO{\cdot}6Al_2O_3$), CA_2 ($CaO{\cdot}2Al_2O_3$), and spinel phase in samples with lower $CaCO_3$ content. With increasing sintering temperatures, the compositions with lower $CaCO_3$ contents gradually achieved maximum densities. Wang et al.[10] sintered AlN with 0.5–3 wt.% $CaCN_2$ and observed similar tendencies with the density increasing with additive content and sintering temperature. Maximum densities however were achieved only above 1700 °C. No second-phase was detected by XRD analysis, but TEM analysis showed a crystalline phase at the grain boundaries, identified as C_3A ($3CaO{\cdot}Al_2O_3$). Multicomponent additive systems, generally including CaO, have also been proposed and sintering temperature as low as 1550 °C has been reported.[11–17] Some of them,[11,12] however, use SiO_2 as a component, which seems to be deleterious to thermal conductivity of AlN.[8,18] In Al_2O_3–CaO system, the lowest eutectic temperatures are around 1400 °C, related to the $C_{12}A_7$ ($12CaO{\cdot}7Al_2O_3$) phase.[19] There is indication that this temperature can be lower with nitrogen in solution.[14] Densification of AlN with CaO has been observed to start between ~1300 and 1500 °C using dilatometer.[14,20,21] It is expected that AlN can achieve high densities at low sintering temperatures, above ~1400 °C, with the addition of only CaO. In fact, Streicher et al.[12] observed that AlN sintered with 0.5 wt.% $CaCO_3$ achieved near theoretical density at 1650 °C. However, increasing the $CaCO_3$ content up to 6 wt.% led to a continuously decreasing sintered densities. This result is opposite to the tendencies depicted above and the authors did not explain it. Jarrige et al.[13] observed similar results of decreasing relative density with increasing additive content for AlN sintered with 2–10 wt.% of CaO, Y_2O_3, and $CaO + Y_2O_3$. Using 1–10 wt.% $CaYAlO_4$, they observed a peak of maximum density with 2 wt.% additive after sintering at 1600 °C, and XRD results revealed for lower additive contents CA_6 and CA_2 phases and for higher additive contents CA, $C_{12}A_7$, and $CaYAl_3O_7$ phases. They pointed out that the decrease in density seemed to be contradictory with the secondary phases formed, since the last phases would be liquid at the sintering temperature. They proposed that high viscosity and low wetting of these phases caused formation of intragglomerate porosity that limited the densification.[13] Hagen et al.[22] further reduced the sintering temperature of AlN using $C_{12}A_7$ as sintering additive. With 8 wt.% $C_{12}A_7$, 97% relative density was achieved at 1550 °C, but after long sintering time (24 h). This result seems to be the lowest temperature reported in the literature on sintering of AlN with relative density above 95%, but it is yet 150 °C higher than the lowest eutectic temperature in the Al_2O_3–CaO system. For now, it is not clear if it is possible to further lower the sintering temperature of AlN with addition of Ca compound.

The oxygen content is constant for a given AlN powder raw material, so with increasing CaO content the expected second-phase should change from an Al_2O_3 rich to a CaO rich aluminate. Hafidi et al.[23] observed this trend in hot-pressed AlN with 1–15 wt.% CaO at 1500 and 1650 °C. They observed the formation of all aluminates predicted in Al_2O_3–CaO system, including the metastable C_5A_3 ($5CaO{\cdot}3Al_2O_3$) phase, with composition close to $C_{12}A_7$ phase, and also, for 15 wt.% addition, free CaO phase. Streicher et al.,[12] however, observed only CA phase in AlN sintered with 0.5–6 wt.% $CaCO_3$. They explained that the nature of intergranular phases would not be sensitive to additive content unless extensive reaction can occur with AlN, which was not expected at low sintering temperature (1650 °C).

In order to understand some of the apparent contradictions observed in the literature, we investigated the sintering process of AlN with CaO. The aim of this work was to study the influence of $CaCO_3$ content on the densification behavior of AlN. Samples with up to 13.4 wt.% $CaCO_3$ addition were prepared by pressureless sintering between 1100 and 2000 °C. The second-phases, weight losses, Ca contents, and microstructures of sintered samples were correlated with the densification curves.

2. Experimental

A commercial AlN powder (Tokuyama Soda, Grade F, Japan, 0.92 μm, 0.85 wt.% O) and a reagent grade $CaCO_3$ (Anidrol Produtos Químicos, Brazil, 5.6 μm) were used as raw materials. Mixtures of AlN with 0.9–13.5 wt.% $CaCO_3$ (corresponding to 0.5–8 wt.% CaO) were prepared. A binder (PEG) was added for each mixture in amount of 2% over total mass. The mixtures were ball milled using plastic jar and balls in isopropyl alcohol for 24 h in order to avoid oxygen contamination. A control sample, AlN with no sintering additive, was also prepared following the same procedure. Each batch was prepared with 100 g powder mixture. Granulated powders were uniaxially pressed at 10 MPa in a cylindrical WC die with 15 mm diameter and then CIPed at 150 MPa forming disk shaped green specimens with 5 mm thickness. Three specimens were prepared for each test condition. Green specimens were settled inside a molybdenum crucible over a layer of pure AlN powder with their planar surfaces in the vertical position, in order to minimize the contact area between the specimen and powder bed. Molybdenum plates separated the specimen groups with different additive compositions. The specimens were sintered in a tungsten resistance heated furnace (Nems, NM-15, Japan) between 1100 and 2000 °C for 1 h under a flowing high purity nitrogen gas (2 L/min) with a slight overpressure of 15 kPa. During heating stage, the samples were held at 500 °C for 0.5 h to burnout the binder. The heating and cooling rates were 10 and 30 °C/min, respectively. Each sample was identified in accordance to its $CaCO_3$ content as indicated in Table 1.

The density of green specimen was determined from its mass and dimensions and the density of sintered specimen was determined by the Archimedean method using alcohol as immersion liquid. Sintered specimens with open porosity were coated with

Table 1
Sample designation (based on $CaCO_3$ content) and equivalent CaO content, calculated considering that all CO_2 is lost by decomposition of $CaCO_3$

Sample designation	$CaCO_3$ content (wt.%)	Equivalent CaO content (wt.%)
P	0	0
C0.9	0.9	0.5
C1.8	1.8	1.0
C3.5	3.5	2.0
C7.0	7.0	4.0
C13.5	13.5	8.0

a nail varnish and the density was calculated from:

$$\rho = m_{a,s}\left(\frac{m_{a,c} - m_{i,c}}{\rho_{H,T}} - \frac{m_{a,c} - m_{a,s}}{\rho_c}\right)^{-1} \quad (1)$$

where, m is mass with subscripts a and i indicating measurement in air or immersed, respectively, and subscripts c and s indicating mass of the specimen with and without coating, respectively, $\rho_{H,T}$ is the density of alcohol at temperature T, and ρ_c is the density of coating (nail varnish). After density measurement, the specimens were immersed in acetone and ultrasonically cleaned. Density results were expressed as percent of theoretical density (% TD), which was calculated by the rule of mixture for each sample considering 3.261 g/cm^3 as the density of AlN and 3.315 g/cm^3 as the density of CaO. The fraction of weight loss of sintered specimen was calculated based on the weights of sintered and green specimens, subtracting the weight of binder.

Powders, green, and sintered specimens were analyzed by scanning electron microscopy (SEM, Jeol, JSM 6300, Japan) to observe the microstructure, by energy dispersive spectroscopy (EDS, Noran Instruments, USA) to determine the chemical elements of second-phase particles, and by X-ray diffraction analysis (XRD, Rigaku, Rint 2000, Japan) to identify the crystalline phases. Pore size distributions of selected sintered specimens, polished until 1 μm diamond and finished with colloidal silica, were determined using an image analyzer (Leica, QWin, Germany). Chemical analysis by ICP-AES (Seiko, SPS 1700R, Japan) was conducted on some sintered specimens to determine the CaO content.

3. Results

3.1. Characterization of the powders and green compacts

Fig. 1a and b show SEM micrographs of the AlN and $CaCO_3$ powders, respectively. The primary particle size of AlN powder was estimated as 0.6 μm. Agglomerates of needle-like particles with broad size distribution, some achieving around 7 μm, were observed in the $CaCO_3$ powder.

The green density of the powder compacts was ~55% TD for all samples. SEM analysis of the green compacts did not show presence of large intergranule voids or segregation of $CaCO_3$ particles.

3.2. Density, weight loss, and CaO content

Results of density of AlN samples sintered between 1100 and 2000 °C are shown in Fig. 2. Density of sample P, without sintering aid, slowly increased with increasing sintering temperature, achieving almost full density (98.5% TD) at 1950 °C. This result is close to the observed by Drew et al. that sintered the same AlN powder used in this study without additive (99% TD at 1900 °C for 1 h).[24] The addition of only 0.9 wt.% $CaCO_3$ (0.5 wt.% CaO) strongly enhanced the densification of AlN, lowering ~200 °C the temperature to achieve full density. The densification started between 1300 and 1500 °C for all samples with $CaCO_3$ addition, but significant densification was observed above 1500 °C

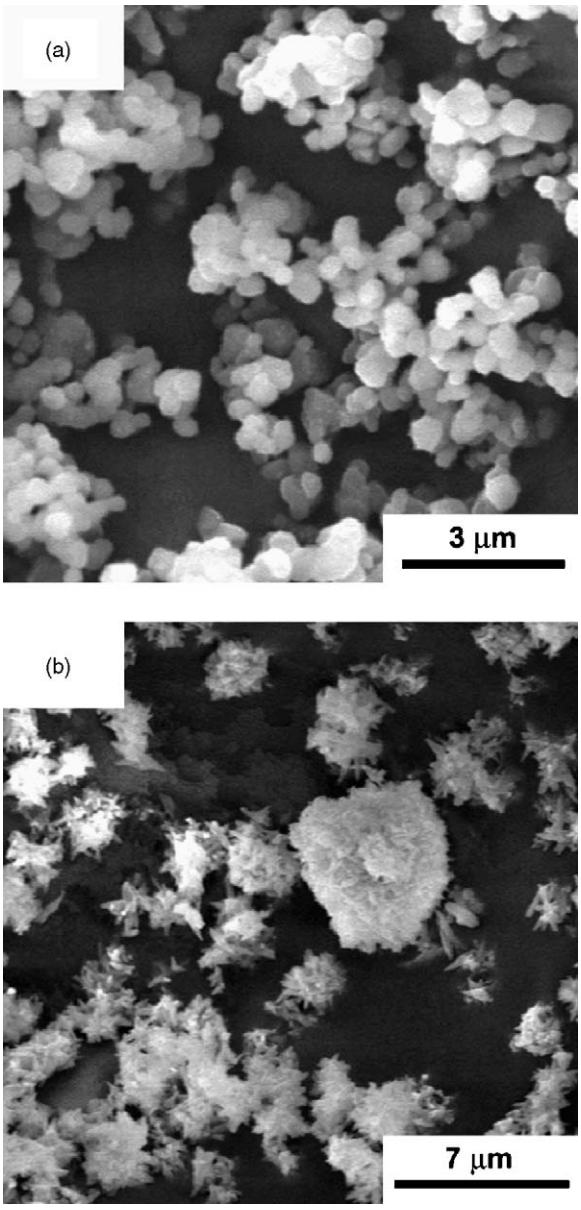

Fig. 1. SEM images of: (a) AlN and (b) $CaCO_3$ powders.

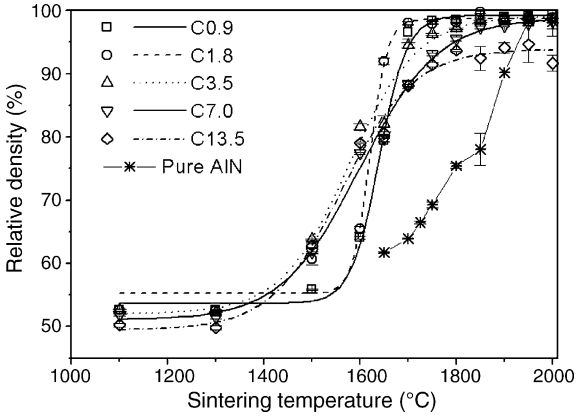

Fig. 2. Relative density versus sintering temperature for "pure" (P) and $CaCO_3$ (C) added AlN samples. The number in sample code indicates the $CaCO_3$ content.

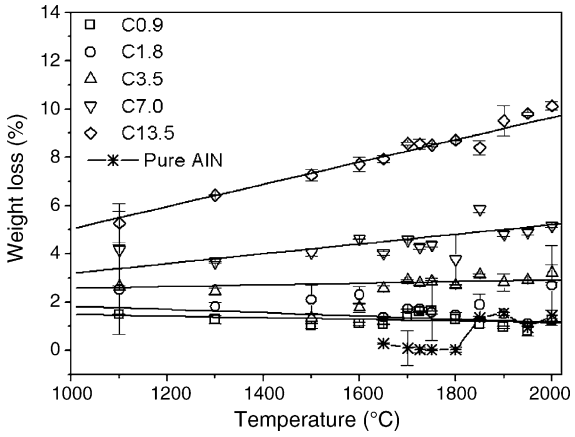

Fig. 3. Weight loss versus sintering temperature for "pure" (P) and $CaCO_3$ (C) added AlN samples. The number in sample code indicates the $CaCO_3$ content.

for samples C3.5, C7.0, and C13.5 and above 1600 °C for samples C0.9 and C1.8.

Samples C0.9 and C1.8 showed rapid increase of density above 1600 °C, achieving full densities at 1750 and 1700 °C, respectively. Their narrow densification curves are indicatives of liquid-phase sintering. For this group, the increase of CaO content enhanced the densification of AlN. Samples C3.5, C7.0, and C13.5 presented higher densities than the sample C1.8 up to 1600 °C, but lower densities above this temperature. For this group, the increase of CaO content retarded the densification of AlN, shifting the densification curve to higher temperatures. Their densification curves were broader than the sintering curves of samples C0.9 and C1.8. Samples C3.5 and C7.0 achieved maximum densities (~98% TD) only at temperatures higher than 1800 °C, because of the slow densification rate above 1700 °C. The density of sample C13.5 achieved ~94% TD at 1800 °C, and remained near constant above this temperature. The specimens of this sample sintered above 1800 °C showed swelling.

Results of weight loss of sintered AlN samples are shown in Fig. 3. The weight loss of the sample P was low (~0.1%) between 1650 and 1800 °C and increased to ~1.4% at 1850 °C. The weight losses of the samples C0.9, C1.8, and C3.5 were almost constant between 1100 and 2000 °C, showing that the weight loss of these samples mostly occurred at low temperatures (at 1100 °C or bellow). Their average values were 1.2, 1.8, and 2.8%, respectively, which were relatively high compared to the added $CaCO_3$ contents. For sample C0.9 the weight loss was higher than the added $CaCO_3$ content and for sample C1.8 it was equal. The values of weight loss of the sample C7.0 slight increased (from ~3.4 to 5.2%) and of the sample C13.5 strong increased (from ~5.4 to 10%) with increasing sintering temperature between 1100 and 2000 °C. All samples showed at 1100 °C weight loss above the expected weight loss of CO_2 from decomposition of $CaCO_3$, indicating that this reaction was mostly completed at 1100 °C and that other components beside CO_2 were evaporated.

Results of CaO content in sintered samples determined by chemical analysis are shown in Fig. 4. The CaO content in samples sintered at 1500 °C varied proportionally to the added

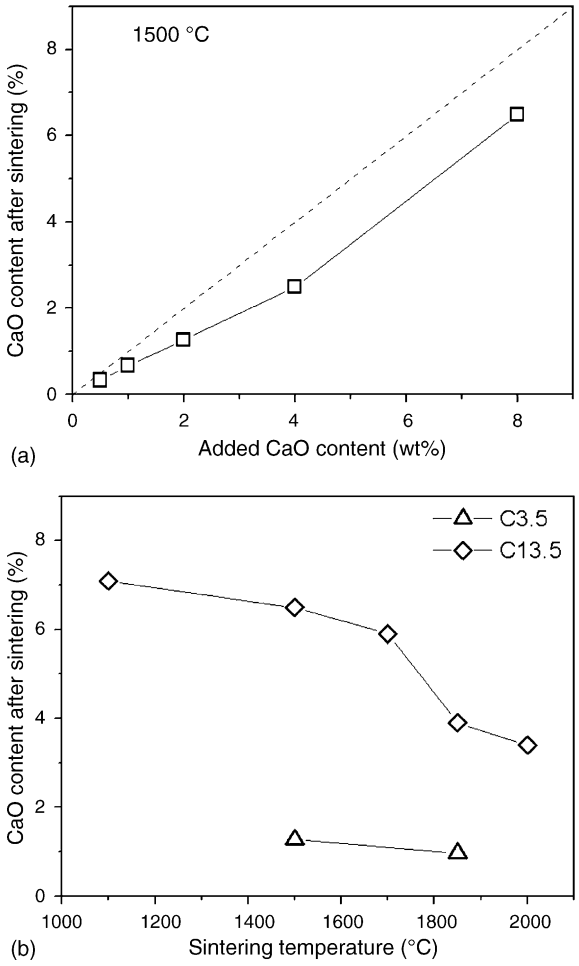

Fig. 4. CaO content in sintered samples: (a) after sintering at 1500 °C versus added $CaCO_3$ content; and (b) for samples C3.5 and C13.5 versus sintering temperature.

$CaCO_3$ content, but the measured values were lower than the added CaO contents (Table 1, dotted line in Fig. 4a). The reduction of CaO content in this temperature was ~34% for samples C0.9 and C1.8, ~37% for samples C3.5 and C7.0, and 19% for sample C13.5. The sample C13.5 showed a decrease of CaO content from 7.1 to 3.4 wt.% with increasing sintering temperature between 1100 and 2000 °C (Fig. 4b), and sample C3.5 showed slight decrease of CaO content from 1.27 to 0.97 wt.% when sintering temperature was raised from 1500 to 1850 °C (Fig. 4b). The reduction of CaO content at 1850 °C was ~50 wt.% for both samples. The correlation between the results of weight loss and CaO content seemed weak. Although for sample C13.5 qualitative inverse correlation was observed between CaO content (Fig. 4b) and weight loss (Fig. 3) with increasing sintering temperature, the rapid decreasing of CaO content between 1700 and 1850 °C was not accompanied by a similar variation of weight loss.

3.3. Secondary phase evolution path

XRD patterns of sample C7.0 sintered at different temperatures are shown in Fig. 5. The main phase identified in all sintered

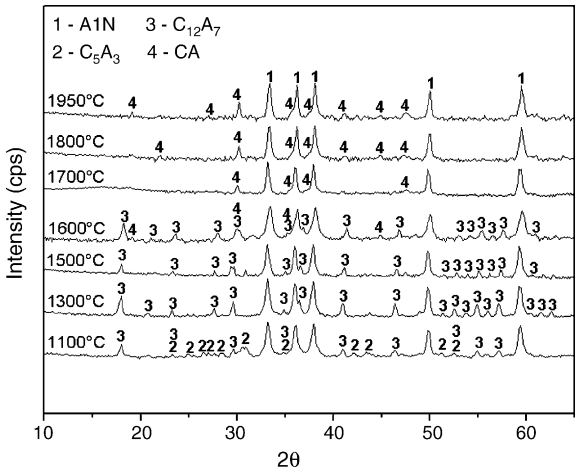

Fig. 5. XRD patterns of sample C7.0 sintered at different temperatures.

samples was AlN and mostly of the second phases were calcium aluminates. Fig. 6 summarizes the results of second-phases identified in the samples sintered between 1100 and 2000 °C. In this figure, some data of the Al_2O_3–CaO phase diagram[19] are shown: the horizontal dashed lines indicate the compositions of calcium aluminate phases and vertical dashed lines indicate the temperatures of invariant reactions with liquid phase.

All samples sintered at 1100 °C showed only calcium aluminate phases, confirming that decomposition of $CaCO_3$ occurred at temperature lower than 1100 °C, in accordance to the results of weight loss (Fig. 3). This result also showed that reaction between CaO and Al_2O_3 (from surface of AlN particles) started at low temperature (1100 °C or bellow).

The evolution of second phase with sintering temperature followed two distinct paths (Fig. 6). For samples with low CaO contents (C0.9 and C1.8), the second phase started as CA at 1100 °C, transformed mainly to CA_2 between 1300 and 1600 °C,

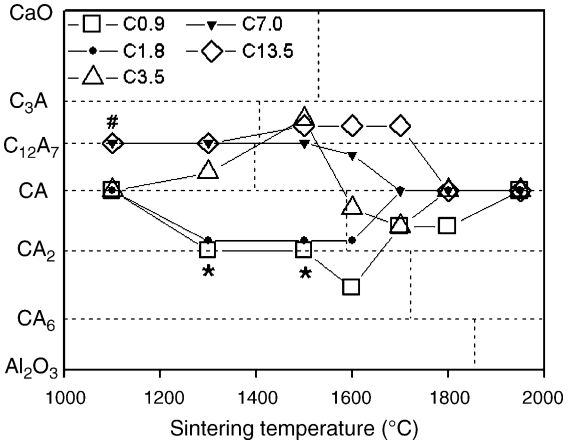

Fig. 6. Secondary phase evolution path diagram for $CaCO_3$ added AlN samples sintered between 1100 and 2000 °C. Horizontal dashed lines indicate the compositions of calcium aluminate phases and vertical dashed lines indicate the temperatures of invariant reactions with liquid phase in the Al_2O_3–CaO system from the equilibrium diagram. The sign (#) indicates the presence of small amount of metastable C_5A_3 phase in sample C7.0, and the sign (*) indicates the presence of minor amount of Al_2O_3 phase in sample C0.9. The number in sample designation indicates the $CaCO_3$ content.

and at higher sintering temperatures, it transformed back to CA. For samples with high CaO contents (C7.0 and C13.5), the second phase was predominantly $C_{12}A_7$ between 1100 °C and 1600 °C (1700 °C for sample C13.5) and transformed to CA above this temperature range. The sample C3.5 showed a tortuous second-phase evolution path, which first approximated the path defined by samples with higher CaO contents, between 1300 and 1500 °C, and then changed at 1600 °C to follow the path of samples with low CaO contents. All samples sintered at 1950 °C showed only CA phase, independent of the initial CaO content.

3.4. Microstructure evolution

Samples C0.9 and C1.8, up to 1600 °C, presented predominantly neck formation between AlN particles (Fig. 7a), indicating that initial densification of around 10% at 1600 °C (Fig. 2) mostly occurred by solid state sintering. At 1650 °C the microstructure changed and significant densification was observed (Fig. 7b). The secondary phase evolution paths of these samples (Fig. 6) indicated liquid phase (L) formation by the eutectic reaction $L \leftrightarrow CA + CA_2$, which is predicted to form above 1589 °C.[19] Probably, the higher liquid phase content of sample C1.8 favored the densification and resulted in almost full dense bodies at 1700 °C (Fig. 7c). At this temperature, sample C0.9 was partially dense (Fig. 7d) and achieved almost full density at 1750 °C (Fig. 7e), in accordance to the results of bulk density (Fig. 2). Residual pores were eliminated with increasing sintering temperature, favored by grain growth (Fig. 7f).

Samples C3.5, C7.0, and C13.5 up to 1300 °C presented predominantly neck formation between AlN particles. Their secondary phase evolution paths (Fig. 6) indicated liquid phase formation by one of the eutectic reactions $L \leftrightarrow CA + C_{12}A_7$ and $L \leftrightarrow C_{12}A_7 + C_3A$, which are predicted to occur above 1396 or 1407 °C, respectively.[19] Agglomerates of AlN particles were observed at 1500 °C (Fig. 8a), showing initiation of liquid-phase sintering process by particle rearrangement mechanism. At 1600 °C, significant localized microstructural densification was observed (Fig. 8b), which evolved to a relatively dense "matrix" of AlN with a dispersion of large pores at 1700 °C (Fig. 8c). The volume fraction of these pores increased with increasing CaO content of the samples (Fig. 8d). Large pores were difficult to eliminate from the microstructure, even after sintering at high temperatures (Fig. 8e). Grain growth favored the shrinkage of the large pores, since it lowered the number of AlN grains surrounding a pore (Fig. 8d–f). The slow bulk densification rates observed in the sintering curves of samples C3.5, C7.0, and C13.5 above 1600 °C (Fig. 2) were controlled by the slow shrinkage rates of the large pores. No large pore was observed in the sample C3.5 sintered at 2000 °C (Fig. 8f), but some residual large pores remained yet in the sample C7.0 sintered at this temperature. In the sample C13.5 sintered above 1800 °C, pore growth and coalescence resulted in the formation of an internal large crack-like defect that caused the swelling of the sintered body and precluded further bulk densification (Fig. 2). Since this sample showed weight loss at high sintering temperatures (Fig. 3), possibly by evaporation, the

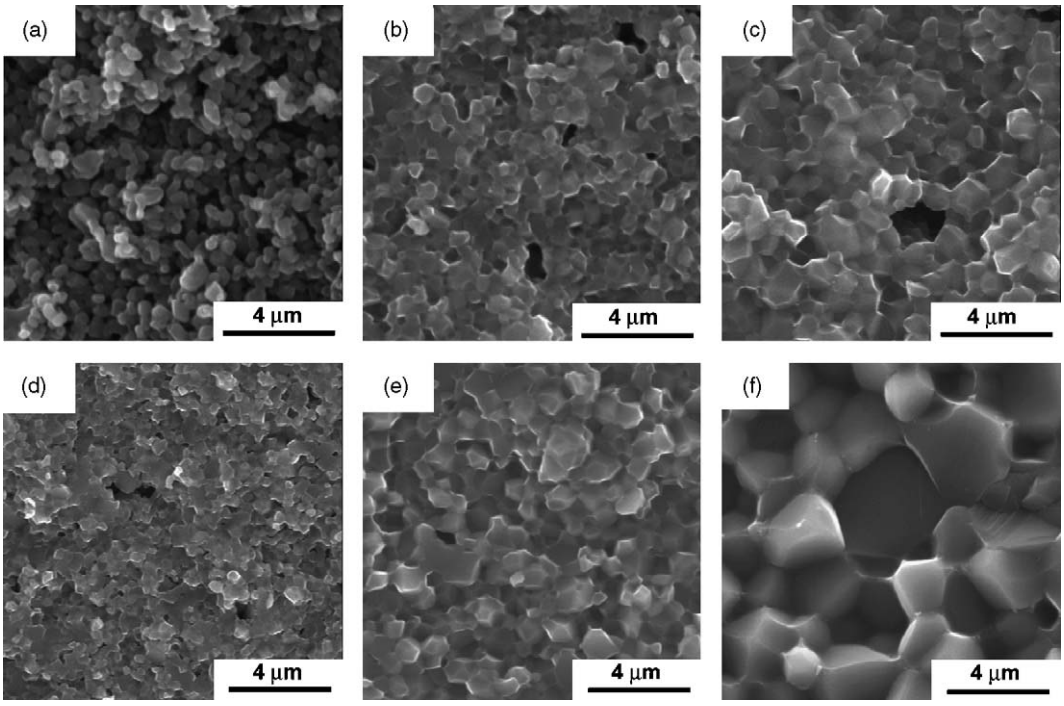

Fig. 7. SEM images of the sample C1.8 sintered at: (a) 1600 °C; (b) 1650 °C; and (c) 1700 °C, and of the sample C0.9 sintered at (d) 1700 °C; (e) 1750 °C; and (f) 2000 °C.

increase of gas pressure inside the pores may have favored the swelling.

Pore size distributions of the samples sintered between 1650 and 1800 °C were determined and typical results are shown in Fig. 9. Samples C0.9 and C1.8 showed average pore size (APS) around 0.3 μm at 1650 °C (Fig. 9a). Increasing sintering temperature to 1750 °C, APS increased to ∼0.8 μm and pore size distribution curve indicated that small pores (<0.5 μm) were significantly reduced. In this temperature range, significant densification by liquid-phase sintering process eliminated preferentially the small pores. At 1800 °C, the intermediate sized pores (∼0.5–1 μm) shrank and APS lowered, but pore size distribution

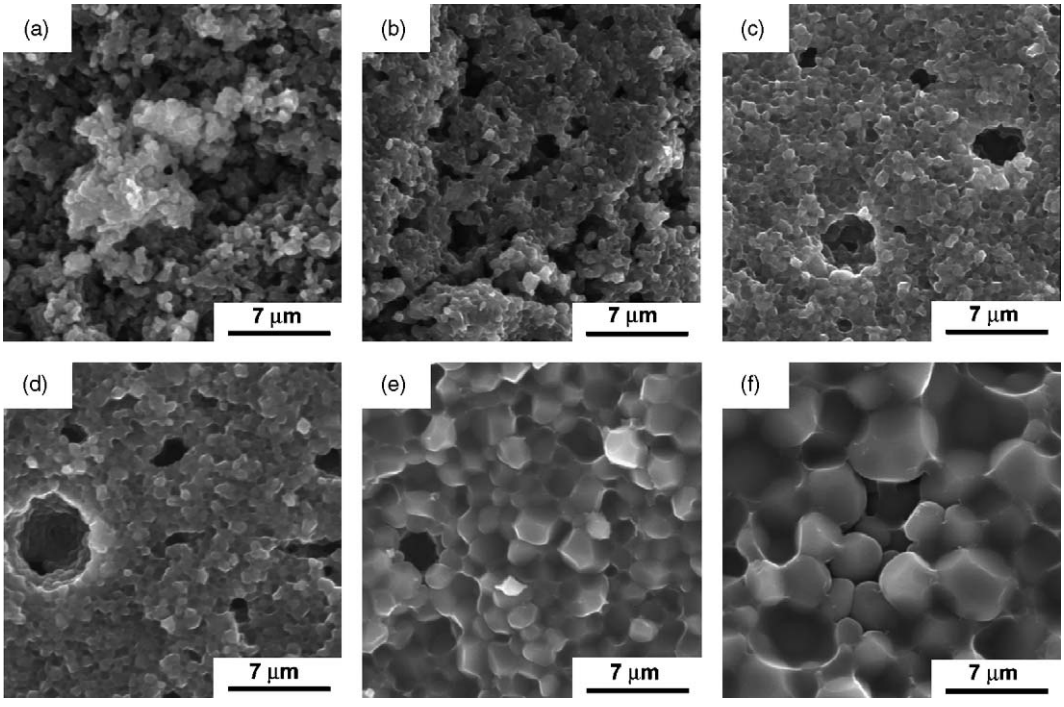

Fig. 8. SEM images of the samples C3.5, C7.0, and C13.5 sintered at different temperatures: (a) C13.5 at 1500 °C; (b) C13.5 at 1600 °C; (c) C3.5 at 1700 °C; (d) C7.0 at 1750 °C; (e) C7.0 at 1900 °C; and (f) C3.5 at 2000 °C.

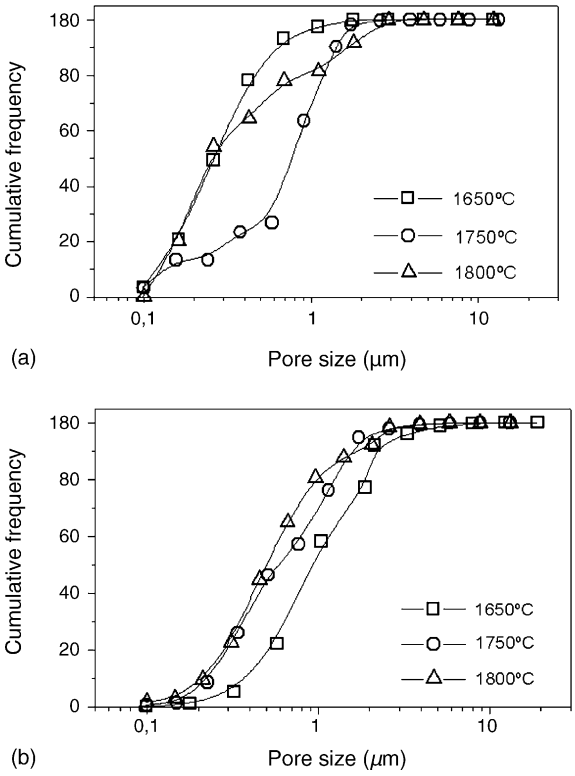

Fig. 9. Pore size distributions of the samples (a) C0.9 and (b) C13.5 sintered at 1650, 1750, and 1800 °C.

curve was broader than that at 1650 °C (Fig. 9a). In comparison, samples C3.5, C7.0, and C13.5 presented at 1650 °C relatively lower fraction of small pores, significantly higher fraction of macropores (>1 μm), and higher APS (∼1 μm, Fig. 9b). The low fraction of small pores is evidence that liquid-phase sintering process was more advanced in these samples at 1650 °C, since localized microstructural densification eliminated rapidly the small pores (Fig. 8b). The high fraction of macropores displaced the pore size distribution curve to large pore size range. With increasing sintering temperature, as the bulk density increased, APS slowly lowered (Fig. 9b).

Observation of the microstructures in sample P, "pure" AlN, sintered between 1650 and 2000 °C, showed the complete absence of large pores. This result reinforces the hypothesis that the large pores were formed in places originally occupied by large $CaCO_3$ particles (Fig. 1b). Decomposition of $CaCO_3$ to CaO first caused particle shrinkage and then the reaction with the AlN particles, adhered to its surface, caused the formation of large calcium aluminate particles detached from the "matrix" of AlN particles (Fig. 10). These particles were observed in the samples C3.5, C7.0, and C13.5 heated up to 1300 °C. At 1500 °C they melted and spread among the AlN particles, emptying the sites they initially occupied. Some remnant particles, however, were also observed in the sample C13.5 at this temperature (Fig. 10c), but not at higher temperatures. Some large pores were also observed in samples C0.9 and C1.8, but they were almost empty at 1100 °C. This result indicates that evaporation of Ca compound could also have formed some of the large pores.

Significantly grain growth started at around 1700 °C, when the samples achieved relatively high densities. No abnormal grain growth was observed in all samples sintered up to 2000 °C. The grain growth rate scaled inversely with $CaCO_3$ content, resulting in larger grain size in samples with lower additive contents (Fig. 7f and Fig. 8f). The fracture surface pattern changed from predominantly transgranular to intergranular mode when AlN grain size achieved around 3 μm, which was at 1750 °C for sample C0.9, 1800 °C for sample C1.8, and 1850 °C for samples C3.5, C7.0, and C13.5.

4. Discussion

The relatively high values of weight loss of the samples C0.9, C1.8, and C3.5 (Fig. 3) indicated that some species other than CO_2 and CaO (or Ca) also evaporated at low temperatures (up to 1100 °C). Since sample P ("pure" AlN) showed only ∼0.1% weight loss up to 1800 °C, it seems that the addition of $CaCO_3$, and the phase transformations related to its decomposition and to the formation of calcium aluminates, caused intense evaporation at low temperatures. The reduction of CaO content during sintering (Fig. 4) can be related to the relatively high vapor pressure of CaO, which is approximately an order higher than the vapor pressure of Al_2O_3 above 1400 °C.[25] Alternatively, Hagen et al.[22] proposed that chemical reactions between AlN and calcium aluminates can generate Ca, Al_2O, and N_2 gaseous species above ∼1600 °C.

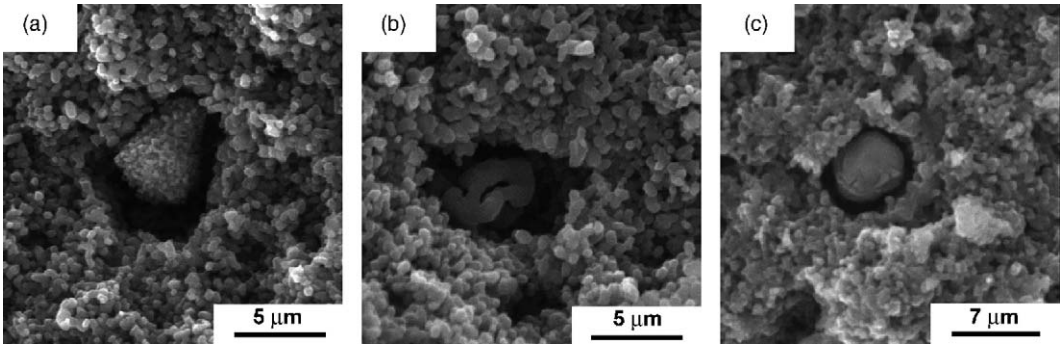

Fig. 10. SEM images showing large particles of calcium aluminates in samples: (a) C3.5 heated at 1100 °C; (b) C7.0 heated at 1300 °C; and (c) C13.5 heated at 1500 °C. EDS analysis of these particles detected high Al, Ca, and O contents.

Considering the Al_2O_3 content of 1.8 wt.% (0.85 wt.% oxygen) in the starting AlN powder and the calculated initial equivalent CaO contents (Table 1), the predicted secondary phases from the powder mixtures for samples C0.9, C1.8, and C3.5 were close to the compositions of CA_2, CA, and $C_{12}A_7$, respectively. For samples C7.0 and C13.5, the calculated compositions lie in the CaO-C_3A two-phase field. In general, however, the second-phases formed between 1300 and 1600 °C (Fig. 6) were poorer in CaO than those predicted from the powder mixtures. This is consistent with the results of chemical analysis, which showed that evaporation of CaO (or Ca) started at low temperatures (Fig. 4), causing the shifting of the second-phase compositions toward Al_2O_3 rich side. This shows that it is difficult to predict the compositions of secondary phases that will be formed during the sintering of AlN, based on the initial contents of CaO and Al_2O_3. Other works have also shown the same trend.[14,22] This occurs because it is difficult to predict the relative loss of the components in the AlN–Al_2O_3–CaO system, which depends on the sintering atmosphere (e.g., flow rate and partial pressure of gas and presence of reducing component as CO in graphite furnace), sintering temperature and time, powder bed composition, crucible material, additive content and type, and so on. It is also possible that the oxygen content increases during AlN powder processing. Because of the difficult to quantify the effects of the above mentioned variables, the diagram of second-phase evolution paths, as shown in Fig. 6, is effective to qualitatively understand and monitor the densification that occurs during the sintering of AlN ceramics.

The secondary phase evolution paths (Fig. 6) indicate some aspects related to the stability of calcium aluminates during sintering of AlN. The phase transformation from CA at 1100 °C to CA_2 at 1300 °C in samples C0.9 and C1.8 indicate that CA phase was metastable at 1100 °C and acted as a precursor for the formation of CA_2 phase. Singh et al.[26] observed that in solid-state reaction between CaO and Al_2O_3 in a molar ratio of 1:2, CaO is rapidly consumed forming CA_2 and CA phases, and afterward CA reacts with the remaining Al_2O_3 to form CA_2. This suggested that some residual Al_2O_3 should exist in these samples at 1100 °C to react with CA. In fact, trace of residual Al_2O_3 phase was observed in the sample C0.9 at 1300 °C (Fig. 6), suggesting that it could also be present at 1100 °C.

The convergence of secondary-phase evolution paths of all samples to CA phase above 1600 °C (Fig. 6) suggested that during sintering of AlN with CaO at high temperatures, a liquid phase with composition of CA phase seems to be more stable than others compositions. For the convergence of the paths to CA phase, the CaO:Al_2O_3 molar ratio of the second-phase should have changed to 1:1 ratio. For samples C0.9 and C1.8, which showed mainly CA_2 phase before the convergence, a reduction of Al_2O_3 content should have occurred. In another hand, for samples C7.0 and C13.5, which showed mainly $C_{12}A_7$ phase before the convergence, a reduction of CaO content should have occurred. Experimentally, a rapid drop of CaO content was observed in the sample C13.5 between 1700 and 1850 °C (Fig. 4b), which is consistent with the change of the second-phase composition in this sample, from $C_{12}A_7$ and C_3A at 1700 °C to CA at 1800 °C (Fig. 6). This result is coherent with the results of Geith et al.[21] that observed, for an AlN sintered with addition of 10 wt.% CaO, second-phase transformation from $C_{12}A_7$ to CA when sintering time was increased from 1 to 3 h at 1750 °C. They also observed that both Ca and O lowered with increasing sintering temperature and soaking time with different evaporation rates, supporting the proposal that the liquid-phase composition can change during sintering. Hagen et al.[22] sintered two AlN powders (fine and coarse, with different oxygen contents) with addition of 4–14 wt.% $C_{12}A_7$ for long sintering time (24 h) between 1550 and 1750 °C in different embeddings, which resulted in different values of weight loss and oxygen content in sintered samples. They observed that the main crystalline secondary phase in all samples was CA, with some samples presenting minor amounts of C_3A and CA_2. Amorphous phase was also observed by TEM analysis. As mentioned before, Streicher et al.[12] also observed only CA phase in AlN sintered at 1650 °C with 0.5–6 wt.% $CaCO_3$. The results indicate that the liquid-phase can achieve CA composition in AlN depending on, at least, the sintering temperature and time. The relative reduction rates of Al_2O_3 and CaO components during liquid-phase sintering of AlN seem to be controlled by the CA composition. Interesting that some of the results mentioned in the introduction section, when AlN with Ca compound achieved high density at relatively low temperatures, CA phase was usually observed after sintering.[9,12,22] Although XRD patterns (Fig. 5) did not show the presence of amorphous phase, TEM studies are necessary to confirm if small amounts of amorphous secondary phases were present or not in the sintered samples in order to confirm that the CA phase is the more stable liquid composition during the sintering of AlN with CaO.

For sample C0.9, the probable reduction of Al_2O_3 favored the occurrence of liquid-phase sintering process above 1600 °C, since at this temperature it presented CA_6 and CA_2 phases (Fig. 6), which eutectic is predicted at 1722 °C.[19] The rapid densification (Fig. 2), microstructure (Fig. 7c), and second-phase evolution path (Fig. 6) of this sample are indicatives that its densification was promoted by liquid-phase sintering process above 1600 °C.

The CA phase in Al_2O_3–CaO phase diagram distinguishes at Al_2O_3 rich side the highest eutectic temperatures and at CaO rich side the lowest eutectic temperatures. Comparing CaO rich samples (C3.5 to C13.5) with Al_2O_3 rich samples (C0.9 and C1.8), showed that formation of calcium aluminates richer in CaO than CA phase ($C_{12}A_7$ and C_3A) promote densification of AlN at lower temperature range than the formation of aluminates richer in Al_2O_3 than CA phase (CA_2 and CA_6). This result was confirmed by densification curves (Fig. 2), second-phase evolution paths (Fig. 6), and microstructure evolutions (Figs. 7 and 8). However, the presence of large pores in samples C3.5, C7.0, and C13.5 (Figs. 8 and 10) retarded the bulk densification. Without them, it would be expect more rapid bulk densification of these samples. In fact, a complementary experiment was conducted with the addition of 2 wt.% CaO powder, obtained by calcination of the $CaCO_3$ powder, and the resultant densification curve was shifted to a temperature range ~50 °C lower than that of the sample C1.8, since large pores were almost absent. This shifting is, however, small compared to the difference between the eutec-

tic temperatures of the two-phase fields CA-CA_2 and CA-$C_{12}A_7$ (or $C_{12}A_7$-C_3A), which is around 200 °C. This occurred because liquid-phase sintering process in AlN with mainly $C_{12}A_7$ phase become significant only at ~1600 °C (Fig. 8b), an overheating of ~200 °C in relation to the $C_{12}A_7$ related eutectic temperatures, while for AlN with mainly CA_2 phase an overheating of only ~60 °C (at 1650 °C), in relation to the CA-CA_2 eutectic temperature, is needed to have extensive operation of liquid-phase sintering processes (Fig. 7b). This shows that, beyond eutectic temperature, the wetting and viscosity of liquid phase are determinant during sintering of AlN with addition of Ca compounds. The strategy to further reduce the sintering temperature of AlN with Ca compounds is to improve the spreading behavior of the liquid-phase with composition near $C_{12}A_7$ in order to enhance the activity of liquid-phase sintering process close to the eutectic temperature. One way to achieve this target was shown by Watari et al., which used a co-doping of Li_2O together with CaO or CaO + Y_2O_3 to lower the sintering temperature of AlN.[14]

In this work, the use of $CaCO_3$ powder with broad particle size distribution (Fig. 1b) and low energy ball milling (plastic jar and balls) favored the formation of large pores. Most of the works in the literature did not measure (or did not attempt to) the size of Ca compound additive. The ball milling with plastic jar and balls was used to mix the AlN and $CaCO_3$ powders in order to avoid oxygen contamination, since the common practice of using Al_2O_3 jar and/or balls can increase the oxygen (or Al_2O_3) content of the powder mixture. The use of $CaCO_3$ with small particle size and narrow size distribution and higher energy milling, accordingly, help avoid or minimize the formation of large pores during sintering of AlN. Since high fractions of large pores were observed in samples C3.5, C7.0, and C13.5 (in proportion to the added $CaCO_3$ content), it seems that liquid-phase sintering process in these samples may have intensified their formation. The melt of large calcium aluminate particles (Fig. 10) and infiltration among AlN particles during the initial stage of liquid-phase sintering may have intensified the particle rearrangement mechanism in the vicinities of large pores, stabilizing or even increasing their sizes. The localized microstructural densification observed in these samples (Fig. 8b) is an indication that formation of large pores was favored by particle rearrangement mechanism through a liquid-phase sintering process. A few large pores were also observed in the samples C0.9 and C1.8 up to ~1750 °C (Fig. 7c and e), but they were smaller and were mostly eliminated at higher sintering temperature. Some sintering characteristics of these samples seem to have acted positively for this microstructural evolution: the densification of ~10% by solid-state sintering; the empty large pores when the liquid-phase sintering process started; their lower liquid-phase fractions, where less densification by particle rearrangement mechanism is expected; and their higher grain growth rates. Although the volume fractions of liquid-phase have not been measured, the higher grain growth rates of theses samples are indicatives that they presented higher fractions of solid-phase.[27]

Residual pores have also been observed in alumina ceramics sintered by liquid-phase sintering process.[28] Ostrowski et al.[29] sintered an Al_2O_3 powder (1 μm) with 8 vol.% of glass powder (2.7 μm) and observed in the microstructure large pores (~10 μm), which they believed to be remnants of initially present large glass particles. Formation of large pores in AlN seems to be a characteristic of $CaCO_3$ addition, and possibly of all Ca compounds, since in the literature, there are references[30–32] showing that AlN sintered with the addition of Y_2O_3 or Y compounds by LPS process presents large yttrium aluminate particles or pockets (5–20 μm), instead of large pores. Both types of defects are undesirable, but large pores can be more deleterious for mechanical strength. Since these pores were not filled by liquid even at high sintering temperature, strict control of particle size distribution of Ca compound is necessary to avoid formation of large pores, which can be deleterious for mechanical strength and reliability even in small fractions.

5. Conclusions

The type of calcium aluminate formed as second-phase in sintered AlN is difficult to be predicted by CaO/Al_2O_3 ratio of raw materials, since it is sensitive to processing route, like CaO loss that occurs during sintering. Evaluation of second-phase evolution path is a suitable approach to help in understanding the densification behavior of AlN with Ca compound additions.

Two microstructural aspects determined the densification of AlN with $CaCO_3$: i) second-phase evolution path; and ii) formation of large pores. Addition of $CaCO_3$ in amounts that form calcium aluminates richer in CaO than CA phase promotes densification at lower temperature range than additions that form aluminates richer in Al_2O_3 than CA phase. The lowering of sintering temperature, however, is lower than the expected difference between the eutectic temperatures, since a higher overheating in relation to the eutectic temperature is need for extensive operation of liquid-phase sintering with calcium aluminates richer in CaO. Large pores are formed in the places originally occupied by large particles of $CaCO_3$. Their formation is favored by particle rearrangement during the initial stage of liquid-phase sintering. The large pores present slow shrinkage rates that retard the bulk densification. Strict control of particle size distribution of Ca compound is necessary to avoid formation of large pores.

Acknowledgements

The authors acknowledge the Brazilian agencies FAPESP and CNPq for the financial support of the present research.

References

1. Sheppard, L. M., Aluminum nitride: a versatile but challenging material. *Am. Ceram. Soc. Bull.*, 1990, **69**(11), 1801–1812.
2. Baik, Y. and Drew, R. A. L., Aluminum nitride: processing and applications. *Key Eng. Mater.*, 1996, **122-124**, 553–570.
3. Komeya, K., Inoue, H. and Tsuge, A., Effect of various additives on sintering of aluminum nitride. *Yogyo-KyoKai-Shi*, 1981, **89**(6), 330–336.
4. Kuramoto, N., Taniguchi, H. and Aso, I., Development of translucent aluminum nitride ceramics. *Am. Ceram. Soc. Bull.*, 1989, **68**(4), 883–887.
5. Slack, G. A., Nonmetallic Crystals with high thermal conductivity. *J. Phys. Chem. Solids*, 1973, **34**, 321–335.

6. Watari, K., Hwang, H. J., Toriyama, M. and Kanzaki, S., Effective sintering aids for low-temperature sintering of AlN ceramics. *J. Mater. Res.*, 1999, **14**(4), 1409–1417.
7. Raghavan, N. S., Pressureless sintering of aluminium nitride: effect of concentration of additives and sintering conditions on properties. *Mater. Sci. Eng.*, 1991, **A148**, 307–317.
8. De Baranda, P. S., Knudsen, A. K. and Ruh, E., Effect of CaO on the thermal conductivity of aluminium nitride. *J. Am. Ceram. Soc.*, 1993, **76**(7), 1751–1760.
9. Komeya, K., Tsuge, A., Inoue, H. and Ohta, H., Effect of $CaCO_3$ addition on the sintering of AlN. *J. Mater. Sci. Lett.*, 1982, **1**, 325–326.
10. Wang, M.-C., Yang, C.-C. and Wu, N.-C., Densification and structural development in the sintering of AlN ceramics with $CaCN_2$ additives. *J. Eur. Ceram. Soc.*, 2001, **21**, 2185–2192.
11. Troczynski, T. B. and Nicholson, P. S., Effect of additive on the pressureless sintering of aluminum nitride between 1500 and 1800 °C. *J. Am. Ceram. Soc.*, 1989, **72**(8), 1488–1491.
12. Streicher, E., Chartier, T., Boch, P., Denonat, M.-F. and Rabier, J., Densification and thermal conductivity of low-sintering-temperature AlN materials. *J. Eur. Ceram. Soc.*, 1990, **6**, 23–29.
13. Jarrige, J., Bouzouita, K., Doradoux, C. and Billy, M., A new method for fabrication of dense aluminium nitride bodies at temperatures as low as 1600 °C. *J. Eur. Ceram. Soc.*, 1993, **12**, 279–285.
14. Watari, K., Valecillos, M. C., Brito, M. E., Toriyama, M. and Kanzaki, S., Densification and thermal conductivity of AlN doped with Y_2O_3, CaO and Li_2O. *J. Am. Ceram. Soc.*, 1996, **79**(12), 3103–3108.
15. Liu, Y., Wu, Y. and Zhou, H., Microstruture of low-temperature sintered AlN. *Mater. Lett.*, 1998, **35**, 232–235.
16. Liu, Y., Zhou, H., Qiao, L. and Wu, L., Low-temperature sintering of aluminum nitride with YF_3-CaF_2 binary additive. *J. Mater. Sci. Lett.*, 1999, **18**, 703–704.
17. Qiao, L., Zhou, H., Xue, H. and Wang, S., Effect of Y_2O_3 on low temperature sintering and thermal conductivity of AlN ceramics. *J. Eur. Ceram. Soc.*, 2003, **23**, 61–67.
18. Yagi, T., Shinozaki, K., Ishizawa, N., Mizutani, N. and Kato, M., Effect of silicon dioxide on the thermal diffusivity of aluminium nitride ceramics. *J. Am. Ceram. Soc.*, 1988, **71**(7), C334–C338.
19. Levin, E. M., Robbins, C. R. and McMuridie, H. F. Supplement phase diagrams for ceramics. *Am. Ceram. Soc.*, 1964, Fig. 2344.
20. Zahneisen, R. and Rüssel, C., Thermal conductivity of calcium-doped aluminium nitride ceramics. Part II. Polymer-derived ceramics. *J. Mater. Sci.*, 1993, **28**, 870–874.
21. Geith, A., Kulig, M., Hofmann, T. and Rüssel, C., Thermal conductivity of calcium-doped aluminium nitride ceramics. Part I. Conventionally produced ceramics. *J. Mater. Sci.*, 1993, **28**, 865–869.
22. Hagen, E., Yu, Y., Grande, T., Hoier, R. and Einarsrud, M.-A., Sintering of AlN using CaO–Al_2O_3 as a sintering additive: chemistry and microstructural development. *J. Am. Ceram. Soc.*, 2002, **85**(12), 2971–2976.
23. Hafidi, A., Billy, M. and Lecompte, J. P., Influence of microstructural parameters on thermal diffusivity of aluminium nitride-based ceramics. *J. Mater. Sci.*, 1992, **27**, 3405–3408.
24. Drew, R. A. L., Baik, Y. and Entezarian, M., Effect of Y_2O_3 content on sintering of aluminum nitride. *Mater. Sci. Forum*, 2000, **325–326**, 249–254.
25. Sata, T., Yoshimura, M., Kuribayashi, K. and Matsumoto, K., Effect of surface sintering on vaporization rate of multicomponent oxide. In *Proceedings of International Symposium on Factors in Densification and Sintering of Oxide and Non-oxide Ceramics*, Ed. S. Somiya and S. Saito, Ookayama, Meguro, Tokyo, 1979. pp. 182–189.
26. Singh, V. K., Ali, M. M. and Mandal, U. K., Formation kinetics of calcium aluminates. *J. Am. Ceram. Soc.*, 1990, **73**(4), 872–876.
27. German, R. M., *Liquid phase sintering*. Plenum Press, New York, 1985, pp 133–143.
28. Price, D. B., *Anorthite development in transient glass phase-processed and 96% alumina ceramics*. M.S. thesis, Colorado School of Mines, USA, March 1994.
29. Ostrowski, T., Ziegler, A., Bordia, R. K. and Rödel, J., Evolution of Young's modulus, strength, and microstructure during liquid-phase sintering. *J. Am. Ceram. Soc.*, 1998, **81**(7), 1852–1860.
30. De Baranda, P. S., Knudsen, A. K. and Ruh, E., Effect of yttria on the thermal conductivity of aluminum nitride. *J. Am. Ceram. Soc.*, 1994, **77**(7), 1846–1850.
31. Kasori, M. and Ueno, F., Thermal conductivity improvement of YAG added AlN ceramics in the grain boundary elimination process. *J. Eur. Ceram. Soc.*, 1995, **15**, 435–443.
32. Hundere, A. M. and Einarsrud, M.-A., Effects of reduction of the Al-Y-O containing secondary phases during sintering of AlN with YF_3 additions. *J. Eur. Ceram. Soc.*, 1996, **16**, 899–906.